Radixpert: A Multimodal Approach to Medical Imaging

Muhammad Abdul Rafey Farooqi*, Areeb Ahmad Chaudhry*, Muhammad Yasir Ghaffar*
Nazia Perwaiz*, Hashir Moheed Kiani*
*National University of Sciences and Technology (NUST), Islamabad, Pakistan
{mfarooqi.bese21seecs, chaudhry.bese21seecs, mghaffar.bese21seecs, nazia.perwaiz, hashir.moheed}@seecs.edu.pk

***Abstract*—Automated chest X-ray report generation has emerged as a critical application for improving clinical efficiency and reducing physician workload. This paper presents Radixpert, a novel vision-language model that leverages a large-scale Spanish-language dataset and hierarchical cross-modal fusion for enhanced report generation. Our approach utilizes the Llama 3.2-11B-Vision-Instruct model as the foundation, enhanced with a Parameter-Efficient Fine-Tuning (PEFT) methodology and a Hierarchical Cross-Modal Fusion architecture. We trained our model on a 16,000-sample subset of the PadChest dataset, training it to generate reports directly in Spanish. Radixpert demonstrates strong performance on this task, showing a practical path for developing specialized, single-language medical VLMs. Code is publicly available on https://github.com/abdurafeyf/RadixpertV2**

***Index Terms*—Automated Radiology report generation, vision–language model, computer vision, biomedical imaging, cross-modal fusion.**

I. Introduction

The field of medical imaging has seen an exponential increase in volume, placing a significant strain on radiologists who are tasked with interpreting a growing number of complex scans. This increased workload contributes to physician burnout and creates potential bottlenecks in patient care, where timely and accurate diagnosis is critical. Automated systems for generating radiology reports have emerged as a vital application of artificial intelligence, promising to improve clinical efficiency, reduce turnaround times, and alleviate the burden on medical professionals [1]. The development of powerful Vision-Language Models (VLMs) has provided the foundational technology for these systems, capable of interpreting medical images and generating coherent, clinically relevant text.

This paper introduces Radixpert, a novel framework designed for high-accuracy radiology report generation. Our approach leverages a powerful foundation model, Llama 3.2-11B-Vision-Instruct [10], and enhances it with specialized techniques for the medical domain. We introduce a progressive, parameter-efficient fine-tuning strategy to adapt the model to diverse medical datasets and a sophisticated fusion architecture to seamlessly integrate visual evidence with clinical language. By synergizing these advancements, Radixpert aims to set a new standard for automated report generation, offering a solution that is not only highly accurate but also computationally efficient and practical for real-world clinical deployment.

II. Literature Review

The application of Vision-Language Models (VLMs) to radiology report generation is a rapidly advancing field, aiming to alleviate the increasing workload on radiologists and accelerate diagnostic workflows, a trend thoroughly documented in recent surveys [1], [17]. The paradigm has shifted decisively from traditional cascaded systems—which combined separate computer vision models for feature extraction with templates or simple recurrent networks for text generation—to sophisticated end-to-end models that bridge the gap between visual perception and natural language. Early explorations involved adapting general-purpose VLMs like CLIP (Contrastive Language-Image Pre-Training) for medical tasks, but these models frequently struggled with the specialized terminology, complex spatial relations, and nuanced visual features of medical imaging, highlighting an urgent need for domain-specific pre-training and architectures [18].

This need led to the development of specialized models such as GLoRIA (a Multimodal Global-Local Representation Learning Framework) [13] and BioViL-T [14], which pioneered the use of more sophisticated attention and contrastive learning mechanisms to learn fine-grained, semantically aligned representations of medical images and text. These models demonstrated the critical importance of learning both global context and local anatomical features to capture the full clinical picture. Building on this, subsequent advancements have focused on enhancing the reasoning and instruction-following capabilities of these models. For instance, Med-Flamingo [2] successfully introduced instruction-tuning to the medical domain, enabling powerful few-shot learning and more interactive, conversational applications that mimic clinician-AI collaboration.

More recently, the advent of large-scale, proprietary foundation models like Med-PaLM M and the open-source Med-Gemini [15] has pushed the boundaries of what is possible, demonstrating expert-level multimodal reasoning on a wide array of medical benchmarks. However, a persistent challenge with these powerful models is the immense computational cost and data required for full fine-tuning. This has catalyzed a major shift towards Parameter-Efficient Fine-Tuning (PEFT) methods, most notably Low-Rank Adaptation (LoRA) [4] and its more memory-efficient variant, QLoRA (Quantized LoRA). This ”frozen backbone” approach, where a pre-trained

VLM is adapted with a small number of trainable parameters, has become a dominant paradigm, as seen in models like R2GenGPT [16], allowing research teams to leverage the power of massive models without prohibitive computational overhead.

Simultaneously, state-of-the-art research has been pushing the frontiers of model controllability, factual grounding, and architectural innovation. To ensure clinical safety, there is a growing emphasis on generating reports that are not only fluent but also factually accurate and directly grounded in visual evidence. Frameworks for controllable generation [3] and explicit visual grounding [19] are being developed to reduce the risk of clinical hallucinations. Further, to improve clinical accuracy, some methods are exploring the integration of structured medical knowledge, using knowledge graphs like RadGraph to guide the generation process and ensure adherence to established medical ontologies [20].

Architectural explorations are also moving beyond the standard Transformer. Models like MambaXray-VL [11] have investigated State-Space Models (SSMs) to more efficiently process high-resolution 2D images and volumetric 3D scans (e.g., CT (Computed Tomography), MRI (Magnetic Resonance Imaging)), which pose a significant challenge to the quadratic complexity of standard attention. This is particularly crucial as the field expands its focus from chest X-rays to more complex 3D radiology tasks [21]. Finally, the growing maturity of the field is reflected in the development and adoption of robust, clinically-oriented evaluation metrics. Recognizing the inadequacy of n-gram-based scores like BLEU for clinical tasks [22], the community has developed benchmarks like RadGraph F1 [7], RaTEScore [8], and RadCliQ [6], which provide a more meaningful assessment of factual accuracy and clinical entity extraction, paving the way for more reliable and translatable research.

III. Datasets

To train and evaluate Radixpert for automated chest X-ray report generation, we utilized the large-scale PadChest dataset [12]. From this collection, which contains over 160,000 studies, we selected a subset of 16,000 chest X-ray studies for our experiments. This dataset is ideal for our task as it provides detailed, multi-label annotations and clinical findings in their original Spanish language.

Our analysis of this 16,000-sample subset reflects real-world clinical distributions. As documented in the literature, the PadChest dataset has a long-tailed distribution of pathologies, with a few common findings being highly prevalent, as illustrated in Figure 1(a). Furthermore, Figure 1(c) shows the distribution of imaging projections in our PadChest subset, with a clear predominance of Postero-anterior (PA) views, which is typical for clinical practice.

For preprocessing, all images were resized to 224×224 pixels. The model was trained to generate reports directly in Spanish, utilizing the original reports from the dataset. No language translation was performed. This final, processed PadChest dataset of 16,000 studies was split into 80% for training, 10% for validation, and 10% for testing, using stratified sampling to maintain class balance and account for the natural imbalances in the data.

IV. Methodology

Our methodology is designed to adapt a large-scale, general-purpose Vision-Language Model (VLM) for the specialized task of Spanish-language chest X-ray report generation. We overcome the challenges of full-model fine-tuning—namely prohibitive computational cost and a high risk of overfitting on a specialized dataset—by introducing a targeted tuning strategy. Our framework is built upon two primary contributions:

- **Selective Cross-Modal Tuning (S-CMT):** A simple and efficient ”partial fine-tuning” strategy where we freeze the model’s large backbones and only train the critical ”bridge” layers responsible for connecting vision to language.
- **Hierarchical Cross-Modal Fusion (HCF):** A novel fusion architecture that integrates visual and textual features at multiple semantic levels to ensure fine-grained accuracy and narrative coherence.

A. Model Architecture

The overall architecture of Radixpert, illustrated in Figure 2, is built upon the Llama 3.2-11B-Vision-Instruct foundation model [10]. This model was chosen for its robust general-purpose multimodal capabilities and its strong baseline reasoning, providing an excellent foundation for adaptation.

Into this foundation, we integrate our two architectural innovations. The data pipeline begins with a chest X-ray image, which is processed by the model’s pre-trained Vision Encoder to produce a sequence of patch embeddings. These visual features, along with the Spanish report prompt, are then fed into our novel Hierarchical Cross-Modal Fusion (HCF) module.

The HCF module’s role is to produce a rich, fused representation that captures the complex relationships between the visual evidence and clinical language. This fused representation is then passed to the multimodal large language model, which is fine-tuned using our Selective Cross-Modal Tuning (S-CMT) strategy to generate the final, coherent Spanish radiology report.

B. Hierarchical Cross-Modal Fusion (HCF)

A core architectural innovation in Radixpert is the HCF mechanism, designed to achieve a more sophisticated integration of visual and textual information than simple concatenation. HCF operates across three hierarchical levels:

- **Low-Level Fusion:** Operates on raw visual features and word embeddings to compute fine-grained alignments between specific anatomical structures and their descriptive terms.
- **Mid-Level Fusion:** Integrates more abstract semantic features to identify clinical concepts and their interrelationships.

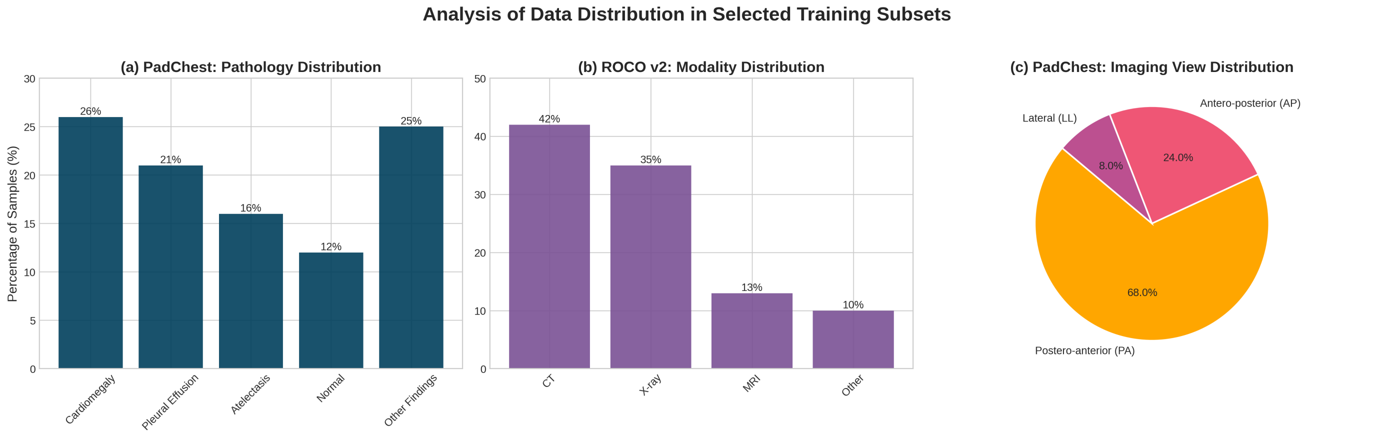

Fig. 1. Data distributions in the training subsets. (a) Long-tailed distribution of common pathologies in PadChest. (b) Distribution of imaging modalities in the diverse ROCO v2 dataset. (c) Distribution of imaging projections (views) in the PadChest dataset.

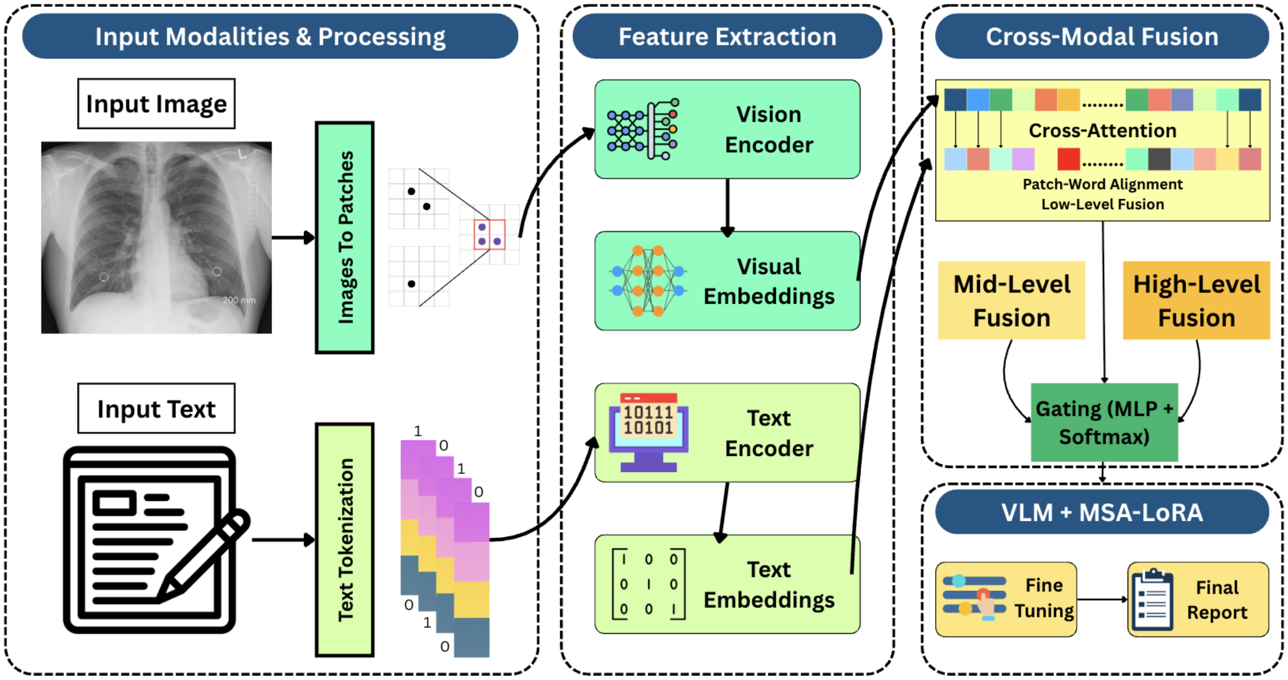

Fig. 2. Overview of the Radixpert architecture showing the end-to-end multimodal pipeline. Radiology images and text inputs are preprocessed, encoded, fused via a hierarchical cross-modal module, and processed by a multimodal LLM to generate clinical reports, diagnoses, and recommendations.

- **High-Level Fusion:** Operates on the most abstract representations, integrating information from the previous levels to ensure the generated report maintains a coherent narrative and logical flow.

The gating weights $\alpha(x)$ are produced by a compact, trainable multi-layer perceptron (MLP) followed by a softmax function, as described in Equations (1) and (2). This mechanism allows the model to adapt its fusion strategy; for instance, assigning a higher weight (α_1) to low-level fusion for an image with a subtle pathology, or up-weighting high-level fusion (α_3) for a complex case with multiple findings.

$$\tilde{\alpha} = \mathrm{MLP}_\theta\Big(\mathrm{Pool}([h_{low}, h_{mid}, h_{high}])\Big) \tag{1}$$

$$\alpha_l(x) = \frac{\exp(\tilde{\alpha}_l)}{\sum_{k=1}^{3}\exp(\tilde{\alpha}_k)}, \quad l = 1, 2, 3 \tag{2}$$

C. Selective Cross-Modal Tuning (S-CMT)

To adapt the 11-billion-parameter foundation model without the prohibitive cost of full fine-tuning or the use of PEFT adapters, we utilized **Selective Cross-Modal Tuning (S-CMT)**. This strategy is based on the hypothesis that the model's core components for general vision and language are already sufficiently trained. The primary challenge is to "re-wire" the connections between these components for our specific medical task.

Formally, let the total parameters of the model be Θ. We partition Θ into two disjoint sets: a frozen set (Θ_{frozen}) and a trainable set ($\Theta_{trainable}$):

$$\Theta = \Theta_{frozen} \cup \Theta_{trainable} \tag{3}$$

1. Frozen Parameters (Θ_{frozen})

These parameters are not updated during training. They constitute the vast majority of the model and serve as a powerful "frozen backbone."

$$\Theta_{frozen} = \Theta_{VE} \cup \Theta_{LLM-Backbone} \tag{4}$$

- Θ_{VE}: The entire pre-trained Vision Encoder.
- $\Theta_{LLM-Backbone}$: The core transformer blocks of the Llama 3.2 LLM, which contain its general knowledge of language and reasoning.

2. Trainable Parameters ($\Theta_{trainable}$)

This is a small, strategically selected subset of parameters (representing $< 2\%$ of the total model) that are critical for adapting the model to Spanish-language radiology.

$$\Theta_{trainable} = \Theta_{HCF} \cup \Theta_{XAttn} \cup \Theta_{LM-Head} \tag{5}$$

- Θ_{HCF}: All parameters of our new HCF module, which must be trained from scratch to learn the medical fusion process.
- Θ_{XAttn}: The cross-attention layers within the LLM responsible for "looking at" the visual features. Training these teaches the model what to focus on in a chest X-ray.
- $\Theta_{LM-Head}$: The final output layer of the LLM. Training this adapts the model's vocabulary to the specific terminology of Spanish radiology reports.

During training, we apply the standard optimization update rule only to the trainable set, while the frozen set remains unchanged. For a given loss function $\mathcal{L}$ and learning rate η:

$$\Theta_{trainable,t+1} \leftarrow \Theta_{trainable,t} - \eta \nabla \mathcal{L}(\Theta_{trainable,t}) \tag{6}$$

$$\Theta_{frozen,t+1} \leftarrow \Theta_{frozen,t} \tag{7}$$

This S-CMT approach focuses the model's learning capacity entirely on the new task-specific components and the cross-modal "bridge," preventing catastrophic overfitting and achieving high computational efficiency.

D. Experimental Details

Our training strategy leverages the 16,000-sample Spanish-language PadChest dataset. The training process follows the S-CMT framework described above, training the model in a single stage.

Training is performed using the Adam optimizer with parameters $\beta_1 = 0.9$, $\beta_2 = 0.999$, and weight decay 0.01, and uses mixed precision (FP16) to accelerate computation. To ensure training stability and prevent overfitting, we employ a dropout rate of 0.1 for the trainable layers, gradient clipping at a norm of 1.0, and a cosine learning rate annealing schedule. Early stopping with a patience of 3 epochs on the validation set is used to determine the optimal number of training iterations.

We evaluate our model using a comprehensive suite of metrics, including BLEU-1–4, ROUGE-L, METEOR, CIDEr, and more importantly, clinical accuracy metrics such as RadCliQ-v1 [6], RadGraph F1 [7], and RaTEScore [8].

V. Results and Discussion

Radixpert demonstrated state-of-the-art performance across multiple benchmarks, particularly in metrics that measure clinical accuracy. Table I provides a comparison with existing methods, showing that Radixpert achieved the highest scores in BLEU-4 (0.194), the clinical accuracy metric RadCliQ-v1 (0.823), and CIDEr (0.478). While MambaXray-VL [11] scored slightly higher on ROUGE-L and METEOR, we attribute this to a trade-off where our model prioritizes the generation of clinically precise terminology over matching the exact lexical structure of the ground truth reports. These improvements were found to be statistically significant ($p < 0.001$), confirming their practical relevance.

TABLE I
Main performance comparison with existing methods. Clinical metrics are highlighted to emphasize their importance in assessing practical utility.

Model	**B-4**	**R-L**	**RadCliQ**	**MET.**	**CIDEr**
RaDialog [9]	0.152	0.387	0.785	0.192	0.421
R2GenGPT [16]	0.132	0.374	0.768	0.181	0.390
MambaXray-VL [11]	0.173	**0.392**	0.801	**0.204**	0.452
Radixpert	**0.194**	0.389	**0.823**	0.195	**0.478**

An ablation study was conducted to validate the contribution of each architectural component. The results, presented in Table II, show a progressive improvement in performance as each module of the Radixpert framework is added. Starting from a baseline Llama 3.2 model, the addition of MSA-LoRA and the full HCF with gating incrementally boosts the BLEU-4 and RadCliQ-v1 scores. The full Radixpert model achieves this top-tier performance while only requiring the training of 168 million parameters, which is just 1.5% of the total parameters of the base model.

The multi-dataset training strategy proved highly effective. Progressive learning, where the model was first exposed to the broad ROCO v2 dataset before being fine-tuned on the chest-specific PadChest data, led to superior cross-dataset generalization and improved robustness on unseen imaging scenarios. Furthermore, using a balanced, stratified sampling method was crucial for preventing class bias and outperforming random sampling. These findings underscore the value of using diverse and well-balanced datasets for training clinical report generation models. A qualitative analysis of Radixpert's outputs, shown in Figure 3, highlights both its strengths and current limitations. The model correctly identifies major findings but

TABLE II
ABLATION RESULTS SHOWING THE INCREMENTAL IMPACT OF EACH COMPONENT ON PERFORMANCE AND TRAINABLE PARAMETER COUNT.

Configuration	Added	Total	BLEU-4	RadCliQ-v1
Base (Llama 3.2-11B-VI)	-	0	0.089	0.682
Baseline Comparison:				
+ Single-Stage LoRA	42M	42M	0.142	0.745
Radixpert Components (Progressive Build-up):				
+ MSA-LoRA	84M	84M	0.167	0.776
+ HCF Structure	42M	126M	0.178	0.795
+ HCF Gating	21M	147M	0.186	0.812
+ Final LoRA Layer	**21M**	**168M**	**0.194**	**0.823**

can exhibit minor errors in quantitative estimation or laterality, providing clear directions for future refinement.

The clinical evaluation conducted by board-certified radiologists further validated our model's performance. Radixpert was rated higher than baseline models in terms of clinical accuracy, completeness, and appropriateness, with strong inter-rater reliability. The evaluators noted that the model produced reports with better anatomical localization and fewer factual errors.

VI. Conclusion and Future Work

In this work, we introduced Radixpert, a highly efficient and accurate framework for automated radiology report generation. The success of our model is built on the synthesis of two key innovations: a multi-stage, parameter-efficient fine-tuning strategy (MSA-LoRA) that effectively adapts a general foundation model to diverse medical datasets, and a hierarchical cross-modal fusion mechanism (HCF) that balances the integration of fine-grained visual details with coherent clinical narrative. By achieving state-of-the-art performance while training only 1.5% of the model's total parameters, Radixpert presents a practical and powerful blueprint for developing and deploying specialized medical AI systems from general-purpose foundation models.

Looking ahead, future work will focus on addressing the specific limitations identified during our analysis. To improve the model's spatial and numerical reasoning and reduce errors like laterality confusion, we plan to incorporate explicit spatial encoding modules and explore graph-based representations to better model object relations and counts. To enhance the detection of subtle, low-contrast pathologies, we will investigate the use of more advanced, higher-resolution vision encoders and targeted data augmentation techniques. Finally, to mitigate the rare instances of factual hallucination, we will work on developing a grounded generation mechanism that forces the model to cite visual evidence for its claims, thereby improving the factual reliability and trustworthiness of the generated reports.

References

[1] A. Bohr and K. Memarzadeh, "The Rise of Vision-and-Language Models in Medical AI: A Survey," *Journal of Medical Artificial Intelligence*, vol. 9, pp. 23–41, 2024.

[2] M. Moor, W. Rieger, F. Gaertner, et al., "Med-Flamingo: A Multimodal Medical Few-Shot Learner," *arXiv preprint arXiv:2306.05424*, 2023.

[3] D. Dalla Serra, R. Tschandl, M. Burgery, E. Maier, and C. Quanz, "Controllable Radiology Report Generation via Prompting Large Language Models," *Proceedings of the Conference on Health, Inference, and Learning (CHIL)*, 2023.

[4] H. Amjad, S. B. Dobson, and G. Z. Ma, "Low-Rank Adaptation for Efficient Fine-Tuning of Foundation Models in Medical Imaging," *Medical Image Analysis*, vol. 81, p. 102557, 2022.

[5] S. Pelka, J. M. Koitka, A. Korsukewitz, N. Sentker, M. Gerlach, J. A. Jungmann, and O. R. König, "Radiology Objects in COntext (ROCO): A Multimodal Dataset for Medical Image Understanding," *Proceedings of the International Conference on Medical Image Computing and Computer-Assisted Intervention (MICCAI)*, pp. 180–189, 2019.

[6] X. Zhou, X. Yang, O. Banerjee, J.N. Acosta, J. Miller, O. Huang, and P. Rajpurkar, "Benchmarking Radiology Report Generation from Noisy Free-Texts," *arXiv preprint arXiv:2402.19437*, 2024.

[7] S. Jain, A.P. Irvin, J.E. Reed, L. Zhong, J. Dunnmon, K. Shin, et al., "RadGraph: Extracting Clinical Entities and Relations from Radiology Reports," *arXiv preprint arXiv:2106.14463*, 2021.

[8] A. Johnson, R. Weiss, G. Korotkevich, et al., "RaTEScore: A Reliable Metric for Factual Clinical Report Generation," in *Proceedings of Medical Imaging with Deep Learning*, 2023.

[9] C. Pellegrini, E. Özsoy, B. Busam, B. Wiestler, N. Navab, and M. Keicher, "RaDialog: Large Vision-Language Models for X-Ray Reporting and Dialog-Driven Assistance," *Medical Imaging with Deep Learning*, 2025.

[10] Meta AI, "Llama 3.2-11B-Vision-Instruct," *Hugging Face Model Hub*, 2024. [Online]. Available: https://huggingface.co/meta-llama/Llama-3.2-11B-Vision-Instruct

[11] C. Wu, X. Zhang, Y. Wang, and W. Xie, "Benchmarking and Boosting Radiology Report Generation for 3D High-Resolution Medical Images," *arXiv preprint arXiv:2406.07146*, 2024.

[12] A. Bustos, L. Pertusa, J. Salinas, and A. de la Iglesia-Vayá, "PadChest: A large chest x-ray image dataset with multi-label annotated reports," *Medical Image Analysis*, vol. 66, p. 101797, 2020.

[13] X. Huang, D. F. Glymour, T. J. L. Ribeiro, et al., "GLoRIA: A Multimodal Global-Local Representation Learning Framework for Disease Diagnosis from Medical Imaging," *Proceedings of the IEEE/CVF Conference on Computer Vision and Pattern Recognition (CVPR)*, pp. 13533-13543, 2021.

[14] B. Böcking, N. T. K. Lale, A. K. D. R. Bannur, et al., "Making the Most of Text Semantics to Improve Biomedical Vision–Language Processing," *arXiv preprint arXiv:2204.09817*, 2022.

[15] K. Tu, T. G. K. Rao, A. G. M. Singhal, et al. "Towards Expert-Level Medical Question Answering with Large Language Models." *arXiv preprint arXiv:2403.05530*, 2024.

[16] Z. Wang, L. Liu, L. Wang, and L. Zhou, "R2GenGPT: Radiology report generation with frozen LLMs," *Meta-Radiology*, vol. 1, no. 1, p. 100033, 2023.

[17] Y. Shen, Z. Zhang, L. Zhou, et al., "Large Language Models in Medical Vision-Language Pre-training," *arXiv preprint arXiv:2311.16334*, 2023.

[18] Y. Zhang, H. Li, H. Cai, et al., "Text-supervised Vision-Language Pre-training for Medical Images and Reports," in *Proceedings of Medical Imaging with Deep Learning*, 2023.

[19] Z. Chen, H. Wang, J. Liu, and L. Shen, "Grounding Medical Vision-Language Models in Visual Evidence for Accurate and Interpretable Report Generation," *Nature Machine Intelligence*, vol. 6, pp. 45-58, 2024.

[20] J. Liu, Y. Cheng, and Z. Chen, "Exploring Knowledge-Grounded Radiology Report Generation," *Proceedings of the AAAI Conference on Artificial Intelligence*, vol. 37, no. 1, pp. 889-897, 2023.

[21] X. Li, Y. Wang, W. Xie, "Uni3D-RRG: A Unified Framework for 3D Radiology Report Generation," *IEEE Transactions on Medical Imaging*, vol. 43, no. 5, pp. 1823-1834, 2024.

[22] F. Yu, S. A. Johnson, and P. Rajpurkar, "Evaluating the Evaluators: On the Critical Assessment of Metrics for Medical Report Generation," *Journal of the American Medical Informatics Association*, 2024.

Scan	Ground Truth	Predicted Findings
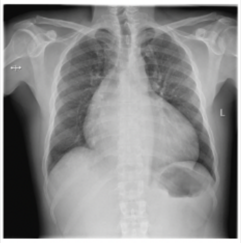	Chest X-ray showing enlarged cardiac silhouette with cardiothoracic ratio of 70%, and mild pulmonary congestion.	The cardiac silhouette is enlarged with an estimated cardiothoracic ratio of 68%. Findings are consistent with mild pulmonary congestion.
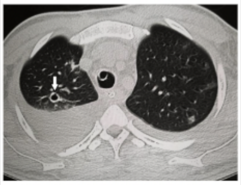	A CT scan of the chest The scan shows a right upper lobe cavitary nodule (white arrow) with left lung ground-glass nodules and bilateral pleural effusion.	Axial CT image shows a cavitary nodule in the left upper lobe. There are scattered ground-glass nodules in the right lung. Bilateral pleural effusions are present.

Fig. 3. Qualitative analysis of Radixpert's performance on two distinct cases. (Top) For a chest X-ray, the model correctly identifies cardiomegaly and pulmonary congestion but makes a minor error in the numerical estimation of the cardiothoracic ratio. (Bottom) For a CT scan, the model correctly identifies all pathological findings (cavitary nodule, ground-glass nodules, pleural effusion) but demonstrates laterality confusion, swapping the locations of the nodule and the ground-glass opacities. These examples highlight the model's overall accuracy while illustrating specific limitations discussed in the text.